tvst

https://doi.org/10.1167/tvst.7.3.20

Article

Characterization of Retinitis Pigmentosa Using Fluorescence Lifetime Imaging Ophthalmoscopy (FLIO)

Karl M. Andersen[1,2,*], Lydia Sauer[1,3,*], Rebekah H. Gensure[1], Martin Hammer[3], and Paul S. Bernstein[1]

[1] John A. Moran Eye Center, University of Utah, Salt Lake City, UT, USA
[2] Geisinger Commonwealth School of Medicine, Scranton, PA, USA
[3] Department of Experimental Ophthalmology, University Hospital Jena, Jena, Germany

Correspondence: Paul S. Bernstein, John A. Moran Eye Center, University of Utah, 65 Mario Capecchi Dr, Salt Lake City, UT 84132, USA. e-mail: paul.bernstein@hsc.utah.edu

Received: 19 December 2017
Accepted: 16 April 2018
Published: 22 June 2018

Keywords: FLIO; fluorescence lifetime imaging; retinitis pigmentosa

Citation: Andersen KM, Sauer L, Gensure RH, Hammer M, Bernstein PS. Characterization of retinitis pigmentosa using fluorescence lifetime imaging ophthalmoscopy (FLIO) Trans Vis Sci Tech. 2018;7(3):20, https://doi.org/10.1167/tvst.7.3.20

Purpose: We investigated fundus autofluorescence (FAF) lifetimes in patients with retinitis pigmentosa (RP) using fluorescence lifetime imaging ophthalmoscopy (FLIO).

Methods: A total of 33 patients (mean age, 40.0 ± 17.0 years) with RP and an age-matched healthy group were included. The Heidelberg FLIO was used to detect FAF decays in short (SSC; 498–560 nm) and long (LSC; 560–720 nm) spectral channels. We investigated a 30° retinal field and calculated the amplitude-weighted mean fluorescence lifetime (τ_m). Additionally, macular pigment measurements, macular optical coherence tomography (OCT) scans, fundus photographs, visual fields, and fluorescein angiograms were recorded. Genetic studies were performed on nearly all patients.

Results: In RP, FLIO shows a typical pattern of prolonged τ_m in atrophic regions in the outer macula (SSC, 419 ± 195 ps; LSC, 401 ± 111 ps). Within the relatively preserved retina in the macular region, ring-shaped patterns were found, most distinctive in patients with autosomal dominant RP inheritance. Mean FAF lifetimes were shortened in rings in the LSC. Central areas remained relatively unaffected.

Conclusions: FLIO uniquely presents a distinct and specific signature in eyes affected with RP. The ring patterns show variations that indicate genetically determined pathologic processes. Shortening of FAF lifetimes in the LSC may indicate disease progression, as was previously demonstrated for Stargardt disease. Therefore, FLIO might be able to indicate disease progression in RP as well.

Translational Relevance: Hyperfluorescent FLIO rings with short FAF lifetimes may provide insight into the pathophysiologic disease status of RP-affected retinas potentially providing a more detailed assessment of disease progression.

Introduction

Retinitis pigmentosa (RP) is a progressive, degenerative disease often presenting early in life. While many patients quickly suffer progression to legal blindness, others retain relatively good central vision for decades.[1,2] Numerous genetic mutations have been identified, resulting in heterogeneity in age at initial onset and symptoms.[3] The genetic mutations invariably lead to nyctalopia, followed by progressive peripheral vision loss.[4] Central vision often remains intact, leading to tunnel-like visual fields with progressive constriction.[5] RP leads to functional impairment of photoreceptors, based on electroretinograms, that often occurs before patients become symptomatic.[6] After initial changes within photoreceptors, the retinal pigment epithelium (RPE) becomes atrophic, resulting in the prototypical peripheral vision loss.[7]

Fundus autofluorescence (FAF) has been used extensively to elucidate the complex progression of RP and propose theories of its etiology.[8,9] It revealed the presence of distinctive hyperfluorescent rings in many patients. Additionally, optical coherence tomography (OCT) images have suggested that this hyperfluorescent ring is an area of active degenera-

Table 1. Characterization of Investigated Groups

	RP	Healthy
Age	40.0 ± 17.0 years	41.7 ± 16.5 years
Range	12 to 77 years	17 to 74 years
Subjects	66 eyes/33 patients	66 eyes/46 subjects
Sex	15 female (45%); 18 male (55%)	23 female (50%); 23 male (50%)
IOL	22 eyes (33%)	4 eyes (6%)

tion. Retinal areas inside the ring (closer to the fovea) are relatively spared, while retinal areas outside the ring (farther from the fovea) show dysfunction due to degeneration of the outer segments of photoreceptor cells.[10] The rings in RP shrink in size as vision is progressively lost over time.[11] Correlating visual fields with FAF in patients with RP suggests that significant damage to the retina already has occurred by the time the hypoautofluorescent peripheral pattern appears in RP.[12] The underlying mechanisms leading to these observed structural changes in RP remain unclear.

Fluorescence lifetime imaging ophthalmoscopy (FLIO) presents as a novel method to characterize molecular changes in retinal diseases.[13] A variety of retinal diseases have been investigated, such as Stargardt disease, age-related macular degeneration, nonproliferative diabetic retinopathy, retinal artery occlusion, choroideremia, central serous chorioretinopathy, macular telangiectasia type 2 (MacTel), macular holes, and Alzheimer's disease.[14–25] FLIO presents a novel way to gain insights into the metabolic changes underlying retinal diseases because fluorescence lifetimes may change with different metabolic states of the retina, likely even before damage is visible.[13,26,27] Recently, characteristic FLIO changes in very early stages of MacTel were reported, and researchers also found that disease progression in Stargardt may be able to be monitored with FLIO.[14,22] In RP, many questions regarding general causes and factors contributing to disease progression remain unanswered. By providing a tool to assess disease activity in vivo, FLIO may help clarify the mechanisms of RP and may also prove valuable in monitoring disease progression.

Methods

This prospective, cross-sectional study was approved by the University of Utah institutional review board (IRB) and adhered to the Declaration of Helsinki. Written informed consent was obtained from all patients before investigations. All patients were examined between March and July 2017 at the Moran Eye Center.

Subjects

We studied 66 eyes of 33 patients with various genetic forms of RP, as well as an age-matched control group recruited from the clinic at the Moran Eye Center (Table 1). One eye from one patient with RP was excluded from analyses due to the presence of lipid crystals in this eye from coexisting Coats reaction, resulting in 65 included eyes with RP. Six of the RP patients regularly consumed lutein supplements (10 mg/day), while the other 27 did not take any supplementation. Compared to the healthy eye group, more patients with RP had undergone cataract surgery. In total, 22 eyes of 11 RP patients had an artificial intraocular lens (IOL). Additionally, two RP patients (4 eyes) had advanced cataracts, and several others had trace cataract. The healthy eyes showed clear, natural lenses or trace cataract. Only four healthy subjects had an IOL. We did not find any significant differences with regard to lens status in any investigated region from either spectral channel (P values ranging from 0.47–0.96).

Genetic testing was performed on all patients except #7 (Bardet-Biedl Syndrome). Thirteen patients possessed autosomal dominant mutations in one of the following genes: *RHO* (five), *PRPF31* (four), *ToPORS* (one), *HK1* (one), *NR2E3* (one), or *PRPH2*-(*RDS*) (one). Among eight patients with autosomal recessive disease, mutations were noted in *USH2A* in three (five eyes), *USH1C* in one, *CRB1* in one, *PDE6B* in one, and *RPGRIP1* in one, and one had Bardet-Biedl syndrome. Additionally, the eyes of two patients with X-linked *RP2* mutations were investigated. In 10 patients, the genetic mutation is currently unknown. Further details on genetic testing, visual acuity, visual fields, and macular edema are presented in Table 2.

Table 2. Characterization of Investigated Individual Subjects

Patient	Age	Sex	Mutation	Inheritance	BCVA	Visual Field (width of III-4e)	Macular Edema
#1	69	F	Unknown	Sporadic	OD: 20/80 OS: 20/70	OU: 20°	N (macular holes bilat)
#2	47	M	*RHO* (G51V)	AD	OD: 20/50 OS: 20/40	OD: 158° OS: 150°	Y (cysts OS)
#3	43	F	*ToPORS* (c.24dupG)	AD	OD: 20/125 OS: 20/50	OU: 16°	N
#4	28	M	Unknown	Sporadic	OD: 20/60 OS: 20/40	OD: 50° OS: 73°	Y (cysts OU)
#5	37	F	*USH2A* (c.2299delG and c.14791+2T>C) OD: Lipid Crystals: eye excluded	AR	OD: count fingers OS: 20/40	OD: 110° (obtained in 2004) OS: 130° (obtained in 2004)	Y (cysts OS)
#6	36	F	Unknown	Sporadic	OD: 20/30 OS: 20/20	OD: 6° OS: 9°	N
#7	16	F	Bardet-Biedl Syndrome, clinical diagnosis only	AR	OU: 20/25	OU: 117°	N
#8	26	F	*USH1C* (c.238dupC and c.760-1G>T)	AR	OU: 20/25	OU: 38°	N
#9	51	F	*USH2A* (c.2299del and c.12575G>A)	AR	OD: 20/100 OS: 20/125	OD: 20° OS: 10°	Y (cysts OU)
#10	38	F	Unknown	Sporadic	OU: 20/30	OD: 30° OS: 44°	N
#11	27	M	Unknown	Sporadic	OD: 20/50 OS: 20/80	OU: 4°	N
#12	31	M	*HK1* (E847K)	AD	OD: 20/20 OS: 20/40	OD: 145° OS: 135°	Y (cysts OU)
#13	58	M	*PRPF31* (c.808dupC)	AD	OD: 20/60 OS: 20/30	OD: 15° OS: 12°	Y (cysts OU)
#14	13	F	*CRB1* (c.3014A>T), homozygous	AR	OD: 20/60 OS: 20/50	OU: 20° centrally; mid-peripheral blind ring of 30°; 150°	Y (cysts OU)
#15	12	M	Unknown	Sporadic	OD: 20/30 OS: 20/40	OU: 120°	N
#16	13	M	Unknown	Apparently sporadic (patient adopted)	OD: 20/20 OS: 20/25	OD: 20° OS: 48°	Y (cysts OS)
#17	42	M	Unknown	Sporadic	OU: count fingers	OD: 4° OS: unable to see III-4e	N
#18	32	M	Unknown	Presumably AR (cousin affected)	OU: 20/80	OD: 18° OS: 16°	N

Table 2. Continued

Patient	Age	Sex	Mutation	Inheritance	BCVA	Visual Field (width of III-4e)	Macular Edema
#19	45	F	*USH2A* (c.2299delG and c.1256G>T)	AR	OU: 20/30	OD: 18° OS: 15°	N
#20	22	M	*RP2* (c.769-33del30)	XL	OD: 20/300 OS: count fingers	OU: 17°	N
#21	21	M	*RP2* (c.769-33del30)	XL	OD: 20/300 OS: 20/500	OU: 19°	N
#22	45	F	*RHO* (G51V)	AD	OU: 20/16	OU: 125°	N
#23	62	M	*PRPF31* (c.808dupC)	AD	OD: 20/50 OS: 20/63	OU: 20°	Y (cysts OS)
#24	35	M	*PRPF31* (R304C and A484G)	AD	OU: 20/32	OU: 40°, temporal crescents	Y (cysts OU)
#25	32	F	*NR2E3* (c.166G>A)	AD	OD: 20/30 OS: 20/60	OD: 116° OS: 98°	Y (cysts OU)
#26	52	F	*PDE6B* (c.1237C>T and c.2399T>C)	AR	OD: 20/200 OS: 20/150	OU: unable to see III-4e	Y (cysts OU)
#27	77	M	Unknown	Sporadic	OD: hand motion OS: 20/30	OD: 17° OS: 40°	N
#28	59	M	*RHO* (c.1040C>T)	AD	OD: 20/20 OS: 20/32	OU: 30°	Y (cysts OU)
#29	40	M	*RHO* (G51V)	AD	OD: 20/50 OS: 20/15	OD: 16° centrally; mid-peripheral blind ring of 45°; 117° OS: 20° centrally; mid-peripheral blind ring of 55°; 120°	N
#30	41	M	*RPGRIP1* (c.673del), second mutation not detected	Probable AR	OD: 20/30 OS: 20/25	OU: 15°	Y (cysts OU)
#31	71	F	*PRPH2 (RDS)* (F211L)	AD	OD: count fingers OS: 20/70	OU: 15°	N
#32	56	M	*PRPF31* (c.808dupC)	AD	OD: 20/50 OS: 20/70	OU: < 5°	Y (cysts OU)
#33	42	M	*RHO* (G51V)	AD	OU: 20/30	OU: 110°	N

OU, *Oculus uterque*.

Procedure

An ophthalmologist examined and diagnosed all patients with RP before inclusion. The best corrected visual acuity (BCVA) was obtained, and pupils were dilated with a drop each of proparacaine, tropicamide, and phenylephrine. FLIO was performed in a dark room with an acquisition time of approximately 2 minutes per eye (minimal signal threshold of 1000 photons for each pixel). Additionally, a spectral

domain (SD)-OCT scan (Spectralis; Heidelberg Engineering, Heidelberg, Germany) of the macula was recorded. Macular pigment was measured with dual wavelength autofluorescence (AFI), which has been described previously.[28] Visual fields (Goldman III-4e) were acquired as well. Genetic testing in CLIA-approved laboratories was performed on almost all patients.

FLIO-Setup and Image Acquisition

The detailed setup and laser safety of FLIO (Heidelberg Engineering) have been described previously.[29–31] FLIO relies on the principle of time-correlated single photon counting.[29,32] It is based on a Heidelberg Spectralis, recording FAF lifetimes from a 30° retinal field centered at the fovea in vivo. FAF is excited by a pulsed diode laser (wavelength, 473 nm; pulse frequency, 80 MHz). Two hybrid photomultipliers (HPM-100-40; Becker&Hickl GmbH, Berlin, Germany) count fluorescence photons, resulting in two separate spectral channels for fluorescence detection: the short (SSC; 498– 560 nm) and long (LSC; 560–720 nm) spectral channels. A photon arrival histogram, representing the probability density function of the decay process, is based on the detection of photons in 1024 time channels. FLIO uses a high-contrast confocal infrared reflectance (IR) image for eye tracking.

The fluorescence data were analyzed using the Software SPC-Image 4.4.2 (Becker&Hickl). The fluorescence decay was approximated by calculating the least-square fit of a series of three exponential functions, and a 3×3 pixel binning was applied. The amplitude weighted mean fluorescence lifetime (τ_m) was used for further analysis, and details have been described previously.[31,32]

Ring-like structures appear in FAF intensity images, but the literature seems to give no uniform definition on the rings. Therefore, we decided to focus on two ring-like structures: the large ring (RL) refers to the hyperfluorescent ring in the peripheral macula, the small ring (RS) refers to the hypofluorescent smaller ring beside it. Masks to determine ring-like structures were drawn according to FAF intensity images. FAF intensity and lifetime images use the same cursor in the SPC-Image software. To obtain interpatient comparable masks, they had to be drawn manually for each eye, as disease stages between patients varied.

The FLIMX software was used for all FAF lifetime analyses and to illustrate the FAF lifetimes.[33] This software is documented and freely available for download online under the open source BSD-license (available in the public domain at http://www.flimx.de).

Statistical Analysis

For all statistical analyses, SPSS 21 (SPSS, Inc, Chicago, IL) was used. To test for significant τ_m differences between regions in one eye, a *t*-test for paired samples was used. To compare data between patients and healthy controls, a *t*-test for independent samples was applied. Data were checked for normal distribution using the Kolmogorov-Smirnov test. For statistical analyses, all study eyes were analyzed separately.

Results

FLIO Characterization of RP Patients

FLIO was used to characterize patterns in RP. Disregarding the genetic background, all patients presented a pattern of significantly prolonged FAF lifetimes in the outer macula. This typical pattern is depicted in Figure 1. Table 3 shows mean FAF lifetimes of defined regions of interest (ROIs), and Figure 2 highlights the ROIs. The outer macula shows FAF lifetimes of 419 ± 195 ps (SSC) and 401 ± 111 ps (LSC) in patients with RP. These times are 154 (SSC) and 119 (LSC) ps longer compared to those of the same region in an age-matched group of healthy eyes ($P < 0.001$).

The mask shown in Figure 2 was projected on each healthy individual, and FAF lifetimes from the same areas were obtained. Although a significant difference was found when comparing the foveal region ("area C") between RP patients and healthy controls, the difference here was only 55 (SSC) and 46 (LSC) ps, with RP patients showing longer FAF lifetimes. We do not consider this difference to be clinically significant in light of the fact that almost all patients had generally spared central vision. The gradient of prolongation was much larger in RP patients for the area of the outer macula, where atrophy presents. This can be seen in the large difference of 154 (SSC) and 119 (LSC) ps. Table 3 shows all data. Figure 3 shows a comparison of mean FAF lifetimes from healthy subjects and patients with RP.

Genetic Phenotypes

Comparing phenotypes of different genetic mutations shows a variety of differences between individuals. Figure 4 gives an overview of characterized

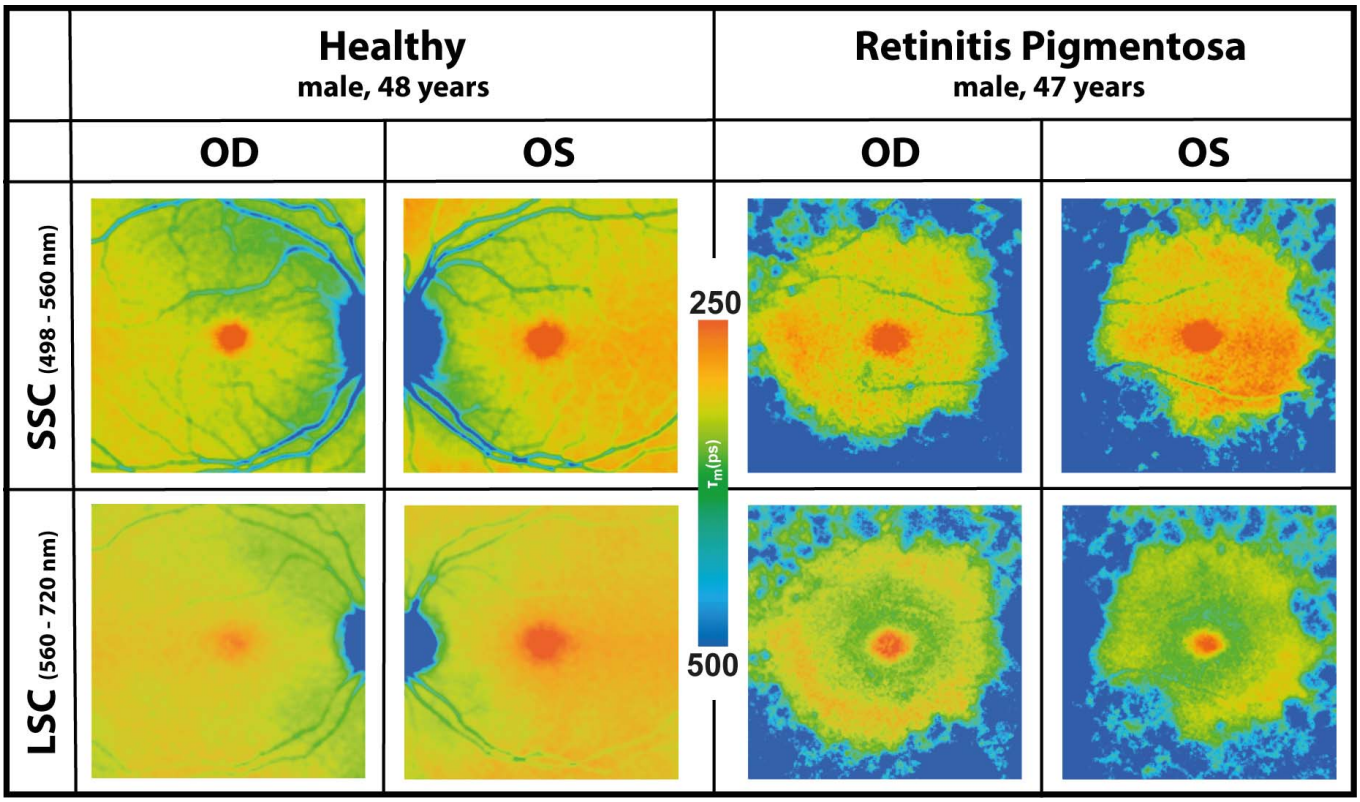

Figure 1. FAF lifetime images from short (SSC) and long (LSC) spectral channels from both eyes (*Oculus dexter* [OD], right; *Oculus sinister* [OS], left) of a healthy subject and a patient with typical features of RP (patient #2).

genetic mutations, based on autosomal dominant (AD) or autosomal recessive (AR) inheritance. We compared 22 patients (43 eyes, one excluded) with defined genetic mutations.

Ring-like Patterns in FLIO and FAF

A ring-like pattern appeared in all eyes with RP, especially pronounced in AD patients and less obvious in AR patients, except for the 4 eyes with X-linked mutations. Also, prolongation in the outer macula was most pronounced in AD genetics. The rings appeared stronger within the LSC (560–720 nm), correlating with findings in FAF intensity images. Figure 5 shows the typical finding of ring-like patterns in FLIO images, Table 3 gives the corresponding τ_m from previously defined specific

Table 3. Mean FAF Lifetimes Over Defined ROIs in Healthy and RP Eyes[a]

	Healthy, ps	RP, ps	Difference, ps	*P* Value
SSC				
Central area (C)	151 ± 54	205 ± 78	55 ± 12	<0.001
Ring small (RS)	222 ± 43	267 ± 78	85 ± 16	<0.001
Ring large (RL)	230 ± 36	254 ± 60	29 ± 10	<0.01
Outer macula (O)	265 ± 53	419 ± 195	154 ± 25	<0.001
LSC				
Central area (C)	218 ± 51	264 ± 60	46 ± 11	<0.001
Ring small (RS)	251 ± 48	325 ± 56	89 ± 14	<0.001
Ring large (RL)	263 ± 45	301 ± 42	40 ± 10	<0.001
Outer macula (O)	282 ± 43	401 ± 111	119 ± 15	<0.001

[a] See Figure 2 for definition of ROIs.

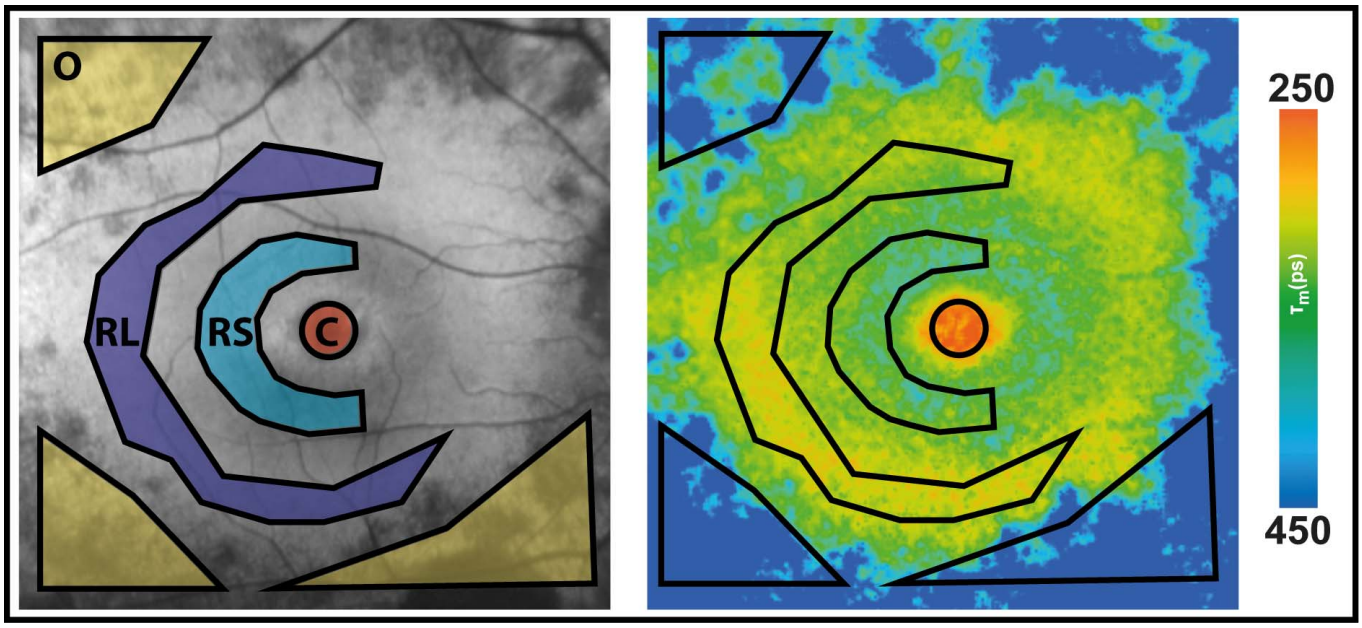

Figure 2. FAF intensity (*left*) and lifetime (*right*) image with ROI to obtain FAF lifetime means, drawn based on FAF intensity image. O, atrophic outer macula; RL, large ring; RS, small ring; C, fovea, central area of a standardized Early Treatment Diabetic Retinopathy Study (ETDRS) grid.

ROIs (see Fig. 2). Mean FAF lifetimes of the ring were 254 ± 60 (SSC) and 301 ± 42 (LSC) ps, which were significantly longer than those of the macular region, but significantly shorter than those of the region of atrophy within the outer macula in both spectral channels ($P < 0.001$). Mean FAF lifetimes in the small ring were significantly longer than those in the large ring (SSC, $P < 0.05$; LSC, $P < 0.001$).

Figure 6 shows how FAF lifetimes differed according to the status of the disease based on visual fields. Whereas some patients (here #2 is depicted) are only mildly affected, others are strongly affected by the disease (here #6 is depicted). FAF lifetimes differ accordingly.

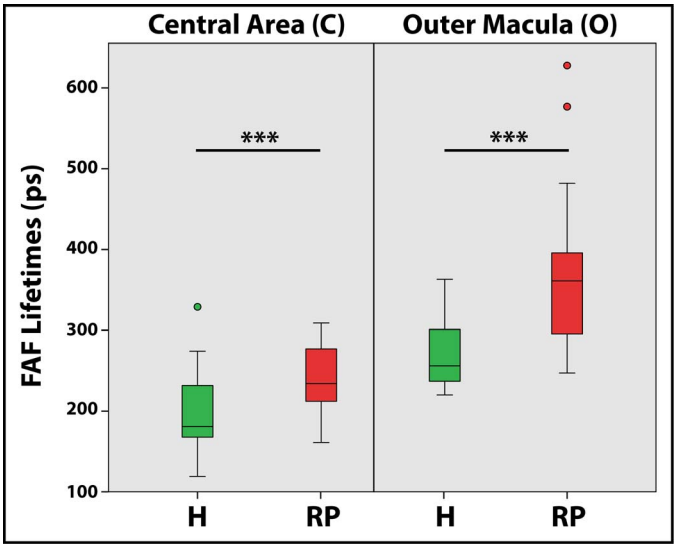

Figure 3. FAF lifetimes from the LSC (560–720 nm) of healthy eyes (H, *green*) and eyes with retinitis pigmentosa (RP, *red*) over defined ROIs. Central area of a standardized Early Treatment Diabetic Retinopathy Study (ETDRS) grid (area C, relating to the fovea) and the outer macula (area O) are presented.

Macular Pigment (MP) in RP

In patients with a spared fovea, the mean MP was found at relatively normal levels. The area of short FAF lifetimes in RP was comparable to that of healthy eyes, although individual foveal lifetimes were slightly longer in RP. The similarity can be seen especially well in the short spectral channel in Figure 1. Eleven eyes showed poor visual acuity (<20/200), indicating significant foveal involvement (see Supplementary Figure S1 for OCT images of all subjects). In these cases, MP did not show normal levels, and all 11 eyes had severe macular thinning rather than macular edema. In supplemented patients, short mean FAF lifetimes in area C were distributed in a larger area, indicating an enhanced accumulation of MP. Supplementation, however, did not prevent the typical RP pattern of prolonged FAF lifetimes in the outer macula from appearing.

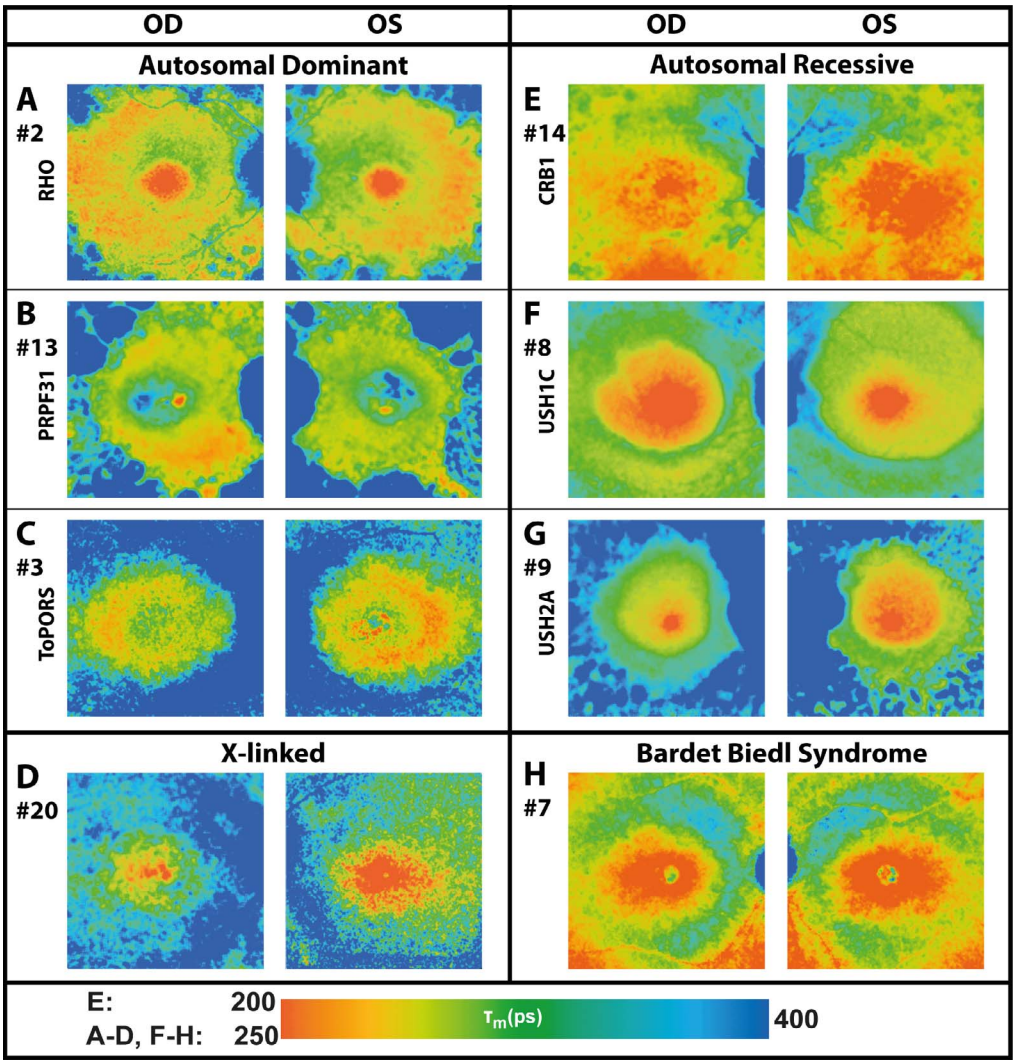

Figure 4. FAF lifetime images from the LSC (560–720 nm) of both eyes from patients with different genetic mutations and RP (patient numbers included). Color ranges were set to comparable means (250–400 ps) for most patients, but were adjusted in one young patient receiving lutein supplementation (*CRB1*; 200–400 ps).

Discussion

In RP, FAF lifetimes showed a typical pattern of prolonged mean autofluorescence decays at the outer macula (area with retinal degeneration). This pattern is very different from the pattern in healthy eyes, which has been described previously.[30,31] The prolongation of τ_m in RP seems to extend beyond the investigated field of 30°, but spares a circular area around the fovea. This area differs in size for each patient. The RP-specific pattern (prolonged τ_m in the periphery) is very typical and can be recognized easily. It relates to retinal atrophy and is in accordance with visual field loss.

Although the majority of cases of RP are associated with genetic variation, the mechanisms of how specific gene defects lead to clinical RP mostly remain uncertain. No sufficient treatment has been found for RP, but a higher intake of vitamin A has been discussed as a protective factor.[34,35] Studies relating to other potential therapeutic approaches are under investigation.[36–43]

Based on extensive genetic research, studies have identified at least 79 genes related to RP.[44,45] The genetic inheritance appears to be 30% to 40% AD (common mutation, rhodopsin (*RHO*) gene, which influences rod function[46]), 50% to 60% AR or sporadic (commonly associated with Usher syndrome type 2, especially the *USH2A* gene), and 5% to 15% X-linked (common mutation, *RPGR* and *RP2*

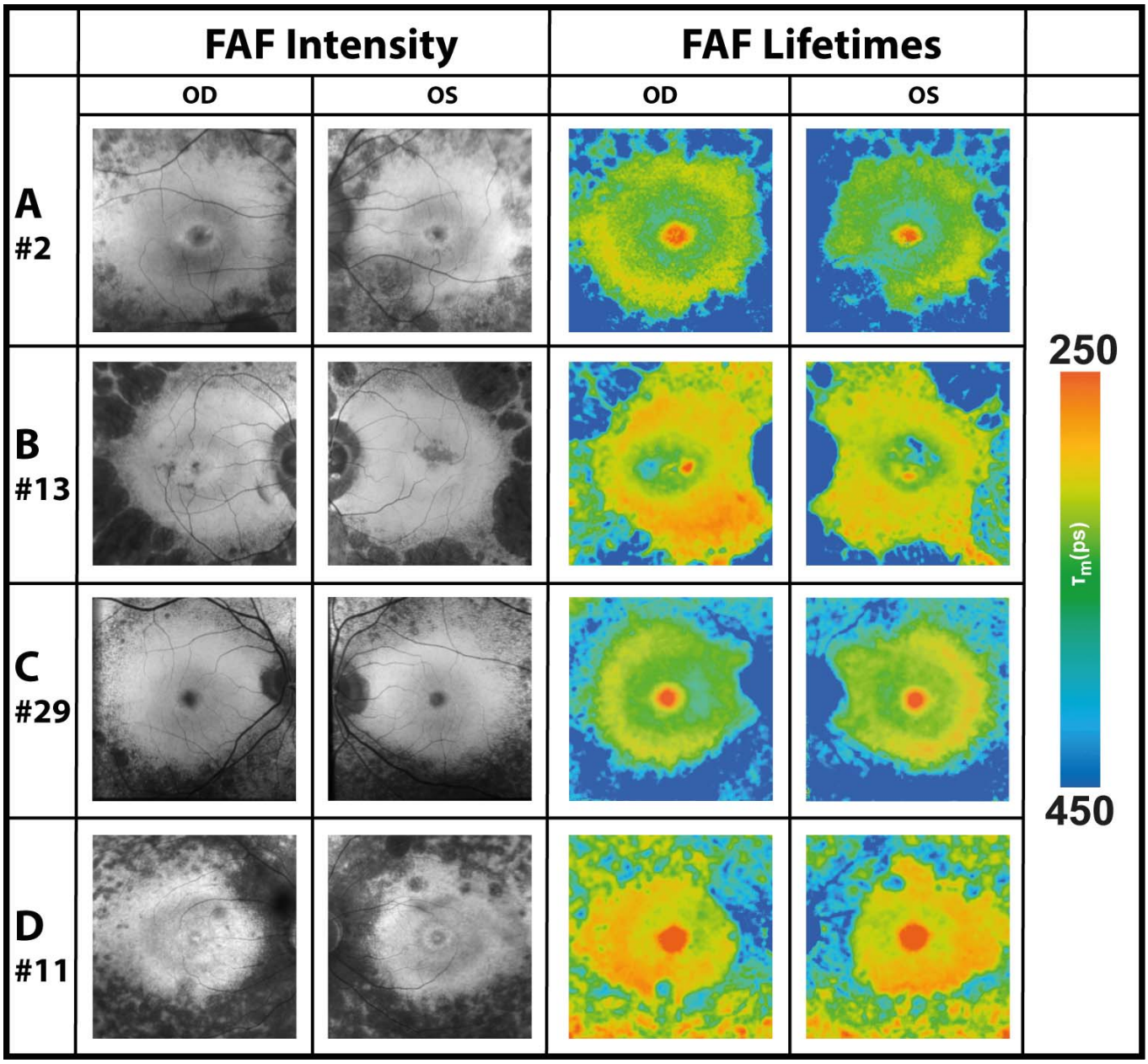

Figure 5. FAF intensity and lifetime images from the LSC (560–720 nm) of four subjects with well-defined rings. Hyperfluorescent rings show short FAF lifetimes (*red color*). All subjects had autosomal dominant inheritance.

genes).[1,46] In this study, we investigated patients with a variety of genetic mutations. Prolongation of τ_m in the outer macula appeared more apparent in AD RP relative to AR RP, reflecting the degree of atrophy in the respective subtypes of RP.

Ring-like patterns, seem to be important in disease progression.[11] Decreased ring size significantly correlates with decreased retinal sensitivity according to BCVA and OCT findings, such as length of the preserved ellipsoid zone (boundary between the inner and outer segments).[11] FAF intensity imaging shows hyperfluorescence at the RP ring, probably caused by lipofuscin, indicating an abnormally increased rate of phagocytosis of degrading photoreceptors.[7] The area of degeneration has been localized precisely to the inner border of the RP autofluorescence ring.[47] Areas peripheral to these rings (in the outer macula) are hypofluorescent due to a loss of RPE and its lipofuscin.[11]

Rings were found in almost all investigated eyes in

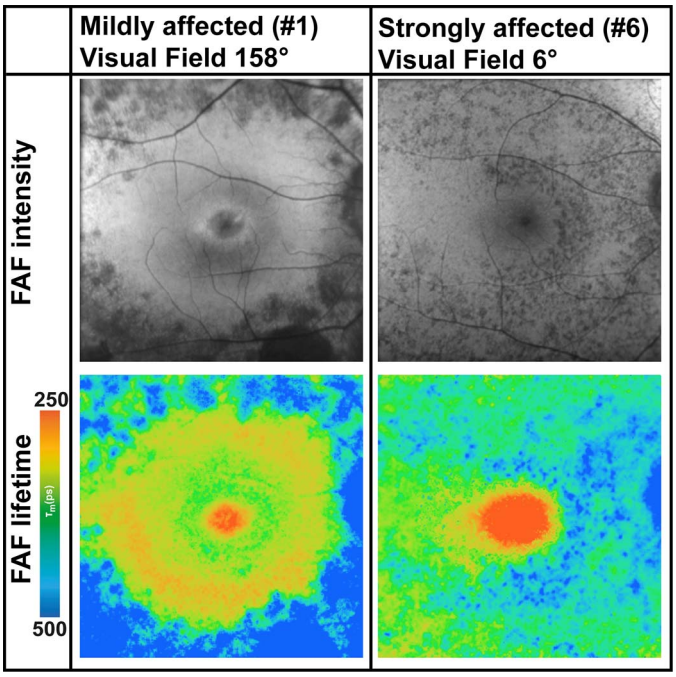

Figure 6. FAF intensity and lifetime images from the LSC (560–720 nm) from two subjects with different disease severities based on the visual field. Whereas patient #2 is only mildly affected, patient #6 is strongly affected.

this study. Interestingly, FLIO adds an extra dimension when investigating the rings. Some rings seem to correlate well with FAF intensity imaging, while others present as quite unique findings. The rings are most apparent within the LSC in patients with AD RP and Usher syndrome. Patients with AR RP still showed clear hyperfluorescent rings, but their FAF lifetime rings were less pronounced. Hyperfluorescent rings in FAF intensity imaging showed short FAF lifetimes. A study focusing on Stargardt disease found that FAF lifetimes of new flecks initially appeared short in the LSC and later shifted to very long FAF lifetimes.[14] Dysli et al.[14] discussed the possibility of monitoring disease progression in Stargardt disease with FLIO. RP presents as a similar retinal degeneration. Therefore, we speculate that in RP as well, short FAF lifetimes in the LSC indicate progression of the disease. Based on these findings,[14] we propose that the ring of short FAF lifetimes demarcates an area of active degeneration within the photoreceptor cells, perhaps even before this presents in other imaging modalities. This finding may be of particular relevance, as some types of RP progress faster than others. To get more detailed insights into how short FAF lifetimes can be related to disease progression, further research and especially longitudinal follow-up investigations are necessary.

In early stages, RP tends to spare the foveal region (defined as a 10° area centered at the fovea), but may eventually also affect this area.[48] Macular pigment levels appeared to be normal in RP-patients with better visual acuity and presumably better fovea preservation. Supplementation with macular carotenoids as a protective approach has been discussed previously, but retinal carotenoid levels of unsupplemented RP patients match those of healthy controls.[49] This is in accordance with our findings. A higher intake of lutein in two of our patients did not prevent typical RP patterns of peripheral/outer macula atrophy developing in their retinas. Reliable MP values were difficult to obtain with the AFI method in our patients, as the reference area for MP often was affected with RPE atrophy. This results in inaccurate calculations when using AFI. Therefore, FLIO is an attractive alternative method to image MP in RP patients, as it does not require a peripheral reference area for calculation. Further details about MP in RP can be found elsewhere.[50]

Differences between the LSC and SSC can be explained by the fact that various chemical substances in the retina fluoresce more dominantly in one channel or the other.[13] The SSC detects photons with a fluorescence emission in the range of 498 to 560 nm, where several retinal fluorophores emit, for example, retinal carotenoids, flavin adenine dinucleotide (FAD), advanced glycation end-products, and collagen/elastin. The LSC has a detection range of 560 to 720 nm and is assumed to be predominantly influenced by the emission of lipofuscin.[23] Additionally, fluorescence lifetimes are relatively independent of the fluorophore's concentration, so that even minor metabolic changes might be detected.

Due to these unique features, FLIO provides information above and beyond FAF intensity imaging. It is a novel method that may detect small molecular changes at the human fundus in vivo. However, the assignment of FAF lifetimes to specific fluorophores is extremely difficult, as FLIO is a noninvasive camera. Further research is necessary to fully understand the additional information of this novel method. Nevertheless, other clinical studies already suggest a strong benefit for the the additional use of FLIO. This technique proved to be useful in monitoring Stargardt disease, MacTel, and AMD.[22,51] We believe that FLIO also provides very useful additional data in RP, which may eventually reveal pathologic and biochemical changes in the

disease and improve the clinical description of disease status.

A limitation of this study lies within differences in the lens status, which may especially influence the SSC. However, we checked for differences in the FLIO data based on IOL versus natural lens and did not find any significant differences or even trends. We assumed the young age of our patients could play a role in this finding. Another limitation lies within the relatively small number of patients in the different genetic subgroups, but overall, 33 total patients still is reasonable for an uncommon disease, such as RP.[52] However, the findings of prolonged FAF lifetimes in the outer macula and rings with short FAF lifetimes appear consistent throughout all patients. We do not think that a larger group of patients would show different results. Further research should be directed to better characterize each individual genetic type of RP. More importantly, longitudinal studies should investigate whether FLIO is a useful tool to predict further retinal atrophy and monitor disease progression.

Conclusion

FLIO characteristics in RP are very consistent across the many genetic forms of RP. All patients with RP show prolonged FAF lifetimes in the outer macula, which seem to spare a ring-like area. The rings as well as the outer macular atrophy appear more apparent in patients with AD inheritance. Based on studies investigating Stargardt disease, we hypothesize that short FAF lifetimes may predict further retinal atrophy. These areas typically correspond to hyperfluorescent rings in FAF intensity images and will be investigated in longitudinal follow-up investigations.

Acknowledgments

The authors thank Heidelberg Engineering for providing the FLIO as well as for their technical assistance. The authors also thank Yoshihiko Katayama, PhD, for his technical assistance, Matthias Klemm, PhD, for providing the FLIMX software, and all coworkers from the John A. Moran Eye Center who helped recruit and image the patients.

Supported by National Institutes of Health (NIH; Bethesda, MD) Grants EY11600 and EY14800 and Research to Prevent Blindness.

Disclosure: **K.M. Andersen**, None; **L. Sauer**, None; **R.H. Gensure**, None; **M. Hammer**, None; **P.S. Bernstein**, None

*KMA and LS contributed equally to this article.

References

1. Hartong DT, Berson EL, Dryja TP. Retinitis pigmentosa. *Lancet*. 2006;368:1795–1809.
2. Shankar S. Hereditary retinal and choroidal dystrophies. In: Rimoin D, Pyeritz R, Korf B, eds. *Emery and Rimoin's Principles and Practice of Medical Genetics*. Cambridge, MA: Academic Press; 2013:1–18.
3. Daiger SP, Bowne SJ, Sullivan LS. Perspective on genes and mutations causing retinitis pigmentosa. *Arch Ophthalmol*. 2007;125:151–158.
4. Fishman GA. Retinitis pigmentosa: visual loss. *Arch Ophthalmol*. 1978;96:1185–1188.
5. Hamel C. Retinitis pigmentosa. *Orphanet J Rare Dis*. 2006;1:40.
6. Berson EL. Retinitis pigmentosa: the Friedenwald lecture. *Invest Ophthalmol Vis Sci*. 1993;34:1659–1676.
7. Murakami T, Akimoto M, Ooto S, et al. Association between abnormal autofluorescence and photoreceptor disorganization in retinitis pigmentosa. *Am J Ophthalmol*. 2008;145:687–694.
8. Schuerch K, Woods RL, Lee W, et al. Quantifying fundus autofluorescence in patients with retinitis pigmentosa. *Invest Ophthalmol Vis Sci*. 2017;58:1843–1855.
9. Jolly JK, Wagner SK, Moules J, et al. A novel method for quantitative serial autofluorescence analysis in retinitis pigmentosa using image characteristics. *Transl Vis Sci Technol*. 2016;5:10.
10. Lima LH, Cella W, Greenstein VC, et al. Structural assessment of hyperautofluorescent ring in patients with retinitis pigmentosa. *Retina*. 2009;29:1025–1031.
11. Aizawa S, Mitamura Y, Hagiwara A, Sugawara T, Yamamoto S. Changes of fundus autofluorescence, photoreceptor inner and outer segment junction line, and visual function in patients with retinitis pigmentosa. *Clin Exp Ophthalmol*. 2010;38:597–604.
12. Oishi A, Ogino K, Makiyama Y, Nakagawa S, Kurimoto M, Yoshimura N. Wide-field fundus autofluorescence imaging of retinitis pigmentosa. *Ophthalmology*. 2013;120:1827–1834.

13. Schweitzer D, Schenke S, Hammer M, et al. Towards metabolic mapping of the human retina. *Microscopy Res Tech*. 2007;70:410–419.
14. Dysli C, Wolf S, Hatz K, Zinkernagel MS. Fluorescence lifetime imaging in stargardt disease: potential marker for disease progression. *Invest Ophthalmol Vis Sci*. 2016;57:832–841.
15. Dysli C, Wolf S, Zinkernagel MS. Fluorescence lifetime imaging in retinal artery occlusion. *Invest Ophthalmol Vis Sci*. 2015;56:3329–3336.
16. Dysli C, Wolf S, Tran HV, Zinkernagel MS. Autofluorescence lifetimes in patients with choroideremia identify photoreceptors in areas with retinal pigment epithelium atrophy. *Invest Ophthalmol Vis Sci*. 2016;57:6714–6721.
17. Dysli C, Wolf S, Zinkernagel MS. Autofluorescence lifetimes in geographic atrophy in patients with age-related macular degeneration. *Invest Ophthalmol Vis Sci*. 2016;57:2479–2487.
18. Dysli C, Berger L, Wolf S, Zinkernagel MS. Fundus autofluorescence lifetimes and central serous chorioretinopathy. *Retina*. 2017;37:2151–2161.
19. Schmidt J, Peters S, Sauer L, et al. Fundus autofluorescence lifetimes are increased in nonproliferative diabetic retinopathy. *Acta Ophthalmol*. 2017;95:33–40.
20. Sauer L, Peters S, Schmidt J, et al. Monitoring macular pigment changes in macular holes using fluorescence lifetime imaging ophthalmoscopy. *Acta Ophthalmol*. 2017;95:481–492.
21. Schweitzer D, Deutsch L, Klemm M, et al. Fluorescence lifetime imaging ophthalmoscopy in type 2 diabetic patients who have no signs of diabetic retinopathy. *J Biomed Opt*. 2015;20:61106.
22. Sauer L, Gensure RH, Hammer M, Bernstein PS. Fluorescence lifetime imaging ophthalmoscopy: a novel way to assess macular telangiectasia type 2. *Ophthalmol Retina*. 2017;2:587–598.
23. Sauer L, Klemm M, Peters S, et al. Monitoring foveal sparing in geographic atrophy with fluorescence lifetime imaging ophthalmoscopy - a novel approach. *Acta Ophthalmol*. 2018:96:257–266.
24. Dysli C, Fink R, Wolf S, Zinkernagel MS. Fluorescence lifetimes of drusen in age-related macular degeneration. *Invest Ophthalmol Vis Sci*. 2017;58:4856–4862.
25. Dysli C, Wolf S, Berezin MY, Sauer L, Hammer M, Zinkernagel MS. Fluorescence lifetime imaging ophthalmoscopy. *Prog Retin Eye Res*. 2017;60:120–143.
26. Schweitzer D. Metabolic mapping. In: Holz F, Spaide R, eds. *Medical Retina*. New York, NY: Springer Berlin Heidelberg; 2010:107–123.
27. Klemm M, Dietzel A, Haueisen J, Nagel E, Hammer M, Schweitzer D. Repeatability of autofluorescence lifetime imaging at the human fundus in healthy volunteers. *Curr Eye Res*. 2013;38:793–801.
28. Dennison JL, Stack J, Beatty S, Nolan JM. Concordance of macular pigment measurements obtained using customized heterochromatic flicker photometry, dual-wavelength autofluorescence, and single-wavelength reflectance. *Exp Eye Res*. 2013;116:190–198.
29. Schweitzer D, Hammer M, Schweitzer F, et al. In vivo measurement of time-resolved autofluorescence at the human fundus. *J Biomed Opt*. 2004;9:1214–1222.
30. Dysli C, Quellec G, Abegg M, et al. Quantitative analysis of fluorescence lifetime measurements of the macula using the fluorescence lifetime imaging ophthalmoscope in healthy subjects. *Invest Ophthalmol Vis Sci*. 2014;55:2106–2113.
31. Sauer L, Schweitzer D, Ramm L, Augsten R, Hammer M, Peters S. Impact of macular pigment on fundus autofluorescence lifetimes. *Invest Ophthalmol Vis Sci*. 2015;56:4668–4679.
32. Becker W. *The bh TCSPC Handbook*, 6th ed. Berlin: Becker & Hickl GmbH; 2014.
33. Klemm M, Schweitzer D, Peters S, Sauer L, Hammer M, Haueisen J. FLIMX: a software package to determine and analyze the fluorescence lifetime in time-resolved fluorescence data from the human eye. *PLoS One*. 2015;10:e0131640.
34. Berson EL, Rosner B, Sandberg MA, et al. A randomized trial of vitamin A and vitamin E supplementation for retinitis pigmentosa. *Arch Ophthalmol*. 1993;111:761–772.
35. Berson EL, Rosner B, Sandberg MA, et al. Vitamin A supplementation for retinitis pigmentosa. *Arch Ophthalmol*. 1993;111:1456–1459.
36. Berger AS, Tezel TH, Del Priore LV, Kaplan HJ. Photoreceptor transplantation in retinitis pigmentosa: short-term follow-up. *Ophthalmology*. 2003;110:383–391.
37. Li LX, Turner JE. Transplantation of retinal pigment epithelial cells to immature and adult rat hosts: short- and long-term survival characteristics. *Exp Eye Res*. 1988;47:771–785.
38. Lin N, Fan W, Sheedlo HJ, Aschenbrenner JE, Turner JE. Photoreceptor repair in response to RPE transplants in RCS rats: outer segment regeneration. *Curr Eye Res*. 1996;15:1069–1077.

39. Little CW, Castillo B, DiLoreto DA, et al. Transplantation of human fetal retinal pigment epithelium rescues photoreceptor cells from degeneration in the royal college of surgeons rat retina. *Invest Ophthalmol Vis Sci*. 1996;37:204–211.
40. Meyer JS, Katz ML, Maruniak JA, Kirk MD. Embryonic stem cell-derived neural progenitors incorporate into degenerating retina and enhance survival of host photoreceptors. *Stem Cells*. 2006; 24:274–283.
41. Seiler MJ, Aramant RB. Transplantation of neuroblastic progenitor cells as a sheet preserves and restores retinal function. *Semin Ophthalmol*. 2005;20:31–42.
42. Whiteley SJ, Litchfield TM, Coffey PJ, Lund RD. Improvement of the pupillary light reflex of royal college of surgeons rats following RPE cell grafts. *Exp Neurol*. 1996;140:100–104.
43. Woch G, Aramant RB, Seiler MJ, Sagdullaev BT, McCall MA. Retinal transplants restore visually evoked responses in rats with photoreceptor degeneration. *Invest Ophthalmol Vis Sci*. 2001; 42:1669–1676.
44. Ferrari S, Di Iorio E, Barbaro V, Ponzin D, Sorrentino FS, Parmeggiani F. Retinitis pigmentosa: genes and disease mechanisms. *Curr Genomics*. 2011;12:238–249.
45. Zhang Q. Retinitis pigmentosa: progress and perspective. *Asia Pac J Ophthalmol (Phila)*. 2016;5:265–271.
46. Yung M, Klufas MA, Sarraf D. Clinical applications of fundus autofluorescence in retinal disease. *Int J Retina Vitreous*. 2016;2:12.
47. Greenstein VC, Duncker T, Holopigian K, et al. Structural and functional changes associated with normal and abnormal fundus autofluorescence in patients with retinitis pigmentosa. *Retina*. 2012; 32:349–357.
48. Holopigian K, Greenstein V, Seiple W, Carr RE. Rates of change differ among measures of visual function in patients with retinitis pigmentosa. *Ophthalmology*. 1996;103:398–405.
49. Zhao DY, Wintch SW, Ermakov IV, Gellermann W, Bernstein PS. Resonance Raman measurement of macular carotenoids in retinal, choroidal, and macular dystrophies. *Arch Ophthalmol*. 2003; 121:967–972.
50. Sauer L, Andersen KM, Li B, Gensure RH, Hammer M, Bernstein PS. Fluorescence lifetime imaging ophthalmoscopy (FLIO) of macular pigment. *Invest Ophthalmol Vis Sci*. In press.
51. Sauer L, Gensure RH, Andersen KM, et al. Patterns of fundus autofluorescence lifetimes in eyes of individuals with non-exudative age-related macular degeneration. *Invest Ophthalmol Vis Sci*. In press.
52. Parmeggiani F. Clinics, epidemiology and genetics of retinitis pigmentosa. *Curr Genomics*. 2011; 12:236–237.